Journal of Nuclear Materials 452 (2014) 31–36

Contents lists available at ScienceDirect

Journal of Nuclear Materials

journal homepage: www.elsevier.com/locate/jnucmat

Investigation of structural stability and magnetic properties of Fe/Ni multilayers irradiated by 300 keV Fe^{10+}

Feida Chen, Xiaobin Tang *, Yahui Yang, Hai Huang, Da Chen

Department of Nuclear Science & Engineering, Nanjing University of Aeronautics and Astronautics, Nanjing, China

ARTICLE INFO

Article history:
Received 23 December 2013
Accepted 26 April 2014
Available online 5 May 2014

ABSTRACT

The effects of irradiation on the structural stability and magnetic properties of Fe/Ni multilayers, which are promising candidate magnet materials in fusion reactors, were investigated. Three types of Fe/Ni multilayers with different modulation periods ranging from 2 nm to 10 nm were deposited on Si (100) substrate through direct current magnetron sputtering. The multilayered samples were irradiated by 300 keV Fe^{10+} ions in a wide fluence range of $1.7 \times 10^{18}/m^2$ to $2 \times 10^{19}/m^2$. Magnetic hysteresis loops of pre- and post-irradiation samples were obtained using a vibrating sample magnetometer, and structural stability were analyzed by X-ray diffraction. Magnetic measurements showed that the coercive force of Fe/Ni multilayers remained stable with increasing irradiation fluence. However, saturation magnetization increased with increasing irradiation fluence. The samples with 5 nm modulation period were the least affected by irradiation among the three types of Fe/Ni multilayers. The effects of temperature during irradiation were also discussed to explore the optimum temperature of multilayers.

1. Introduction

Iron-based multilayers exhibit soft magnetic properties, such as low coercivity and high remanence. These multilayers have important applications in devices, such as hall current sensor [1]. They are also considered candidate first wall materials in fusion reactors [2]. Thus, the effects of irradiation on the structural and magnetic properties of Fe-based multilayers in aggressive environments need to be studied.

Höchbauer et al. [3] suggested that multilayer nanocomposites of metals with immiscible interfaces are great radiation tolerance materials because of the ability of nano-interfaces to mitigate radiation-induced defects and control helium bubble growth. Multilayer nanocomposites, such as Cu/Nb [4–7], Ag/V [8], Cu/W [9], and Fe/Cu [10], have been investigated. The mixing enthalpy values in the solid state of these nanocomposites were calculated to be +3, +17, +22, and +13 kJ/mol, respectively, using Miedema's model [11]. However, most of these nanocomposites are not suitable for nuclear reactor applications if factors, such as induced radioactivity and cost of the composed chemical elements, are considered [12]. Thus, the searching criteria for suitable radiation tolerance materials for nuclear energy applications need to be relaxed abstemiously and the scale-up composite systems with a low negative mixing enthalpy should be included in further studies.

In the present work, we concentrate on the effects of irradiation on the structural stability and magnetic properties of Fe/Ni multilayers, also known as permalloy. The mixing enthalpy of the Fe/Ni system is −2 kJ/mol, which is slightly smaller than that of the Cu/Nb system. The multilayer nanocomposites were irradiated by 300 keV Fe^{10+} ions in a fluence range of 1.7×10^{18} ions/m^2 to 2×10^{19} ions/m^2. The structural and magnetic stability of pre- and post-irradiation samples were characterized via X-ray diffraction (XRD) and vibrating sample magnetometer (VSM), respectively.

2. Experimental

Fe/Ni multilayers were deposited on the monocrystalline Si(100) substrate with a diameter of 38 mm by direct current (DC) magnetron sputtering. The base vacuum was evacuated to a pressure of less than 4×10^{-4} Pa before deposition, and the argon pressure was maintained at 0.5 Pa during the deposition. The deposition rates of Fe and Ni were both approximately 13.6 nm/min at a DC power of 40 W. The layer thicknesses of Fe and Ni varied from 2 nm to 10 nm, whereas the total thickness of each film was approximately 100 nm. After deposition, 1 × 1 cm square pieces were cut apart from the Si substrate using laser from the back side of substrate to refrain from damaging the multilayers. These square piece samples were then irradiated by 300 keV Fe^{10+} ions in a fluence range of 1.7×10^{18} ions/m^2 to 2×10^{19} ions/m^2. Irradiation experiments were performed at the 320 kV platform at the

* Corresponding author. Tel.: +86 13601582233; fax: +86 025 52112906 80407.
E-mail address: tangxiaobin@nuaa.edu.cn (X. Tang).

http://dx.doi.org/10.1016/j.jnucmat.2014.04.039
0022-3115/

Institute of Modern Physics, Chinese Academy of Sciences (CAS). Grazing Incidence X-ray Diffraction (GIXRD) with Cu K_α radiation ($\lambda = 0.154$ nm) was carried out with the incident angle fixed at 0.5° to characterize the structural properties of the pre- and post-irradiation samples. Transmission electron microscopy (TEM, Tecnai G2 F20 S-Twin) was conducted to obtain detailed structural information on the interfaces before and after the ion irradiation. For the section samples preparation, two pieces of a single sample were glued together, sectioned with a wafer saw, mechanically polished to a thickness of about 30 μm, and subsequently ion milled to electron transparency. Vibrating sample magnetometer (VSM) were conducted to characterize the magnetic properties of the samples.

3. Results and discussion

3.1. Dpa distribution calculated using SRIM

We performed self-ion irradiation on the Fe/Ni multilayers to simulate neutron irradiation, considering the huge time consumption of neutron irradiation experiments. Correlation between the ion fluences and material damage degree was calculated using the full-damage cascade mode of SRIM2010 [13]. The implantation of 300 keV Fe^{10+} ions into the three Fe/Ni multilayers was simulated with the modulation period ranging from 2 nm to 10 nm. The total layer thickness of the three multilayers is 100 nm. The displacement energies of Fe and Ni are 17.4 eV and 22 eV, respectively [14].

Fig. 1 shows the dpa distribution of $[Fe(10\ nm)/Ni(10\ nm)]_5$, $[Fe(5\ nm)/Ni(5\ nm)]_{10}$, and $[Fe(2\ nm)/Ni(2\ nm)]_{25}$. The interfaces between each Fe/Ni layer are not marked on Fig. 1(c) because the interval space is very small. Simulation results predict that the damage degrees corresponding to the fluences of 1.7×10^{18}, 1.02×10^{19}, and 2.04×10^{19} ions/m^2 are approximately 1, 6, and 12 dpa, respectively. The modulation period of multilayers does not significantly change the damage distribution in materials.

3.2. Structural stability

Characterization of the individual layer thickness and the distribution of elements of the as-deposited $[Fe(5\ nm)/Ni(5\ nm)]_{10}$ sample was performed by EDX. According to Fig. 2, it's clear that the roughness on the film surface is about 2 nm. Fig. 3 shows the GIXRD curve corresponding to $[Fe(10\ nm)/Ni(10\ nm)]_5$, $[Fe(5\ nm)/Ni(5\ nm)]_{10}$, and $[Fe(2\ nm)/Ni(2\ nm)]_{25}$, as a function of the ion irradiation dose. The intense peaks at 2θ values of 44.604°, 51.977°, and 76.588° represent Ni(111), Ni(200), and Ni(220), respectively. The Fe(110), Fe(200), and Fe(211) peaks are also observed at 2θ values of 44.672°, 65.021°, and 82.333°, respectively. The curve of the as-deposited $[Fe(2\ nm)/Ni(2\ nm)]_{25}$ exhibits a peak at $2\theta = 53.115°$, which is probably the result of the Si(301) substrate. By combining these results with earlier studies [15,16], we can obtain the conclusion that the multilayers are strongly Ni(111)/Fe(110) textured.

The Ni(111)/Fe(110) peak and Ni(200) peak shift toward lower angles as the ion irradiation dose increases. This phenomenon can be observed from 6 dpa curves of $[Fe(10\ nm)/Ni(10\ nm)]_5$ and

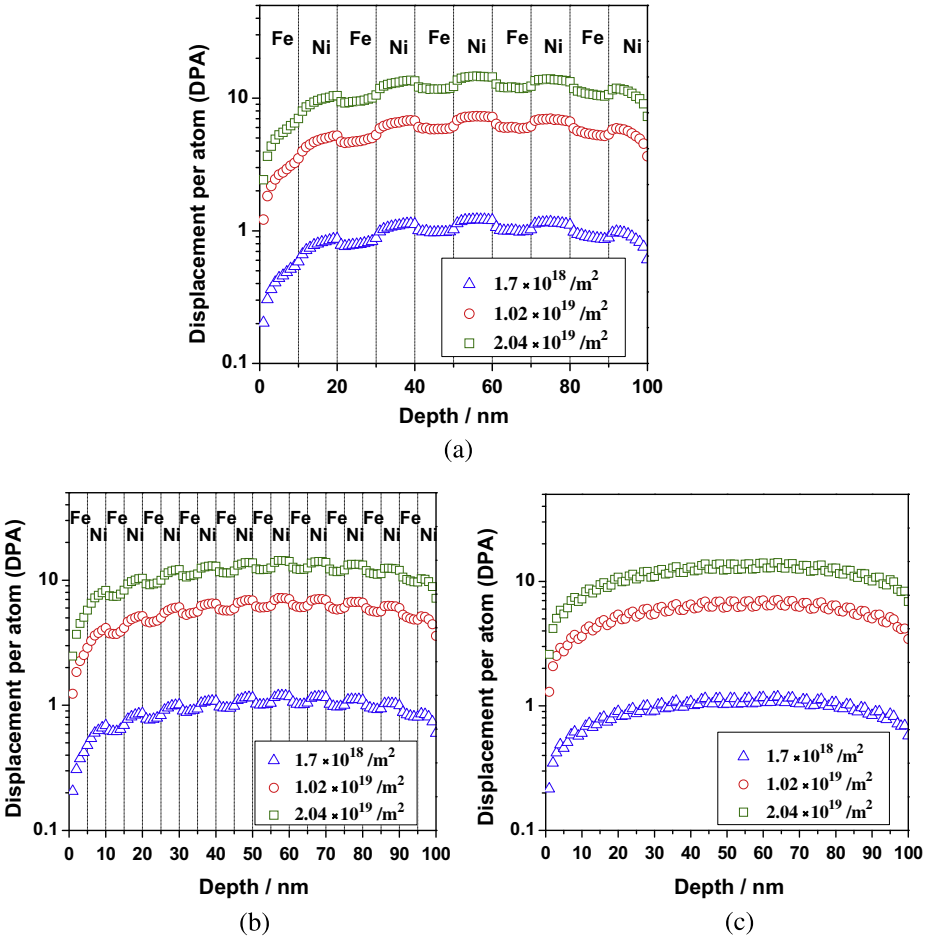

Fig. 1. Depth distribution of dpa induced by 300 keV Fe^{10+} ions: (a) $[Fe(10\ nm)/Ni(10\ nm)]_5$, (b) $[Fe(5\ nm)/Ni(5\ nm)]_{10}$, and (c) $[Fe(2\ nm)/Ni(2\ nm)]_{25}$.

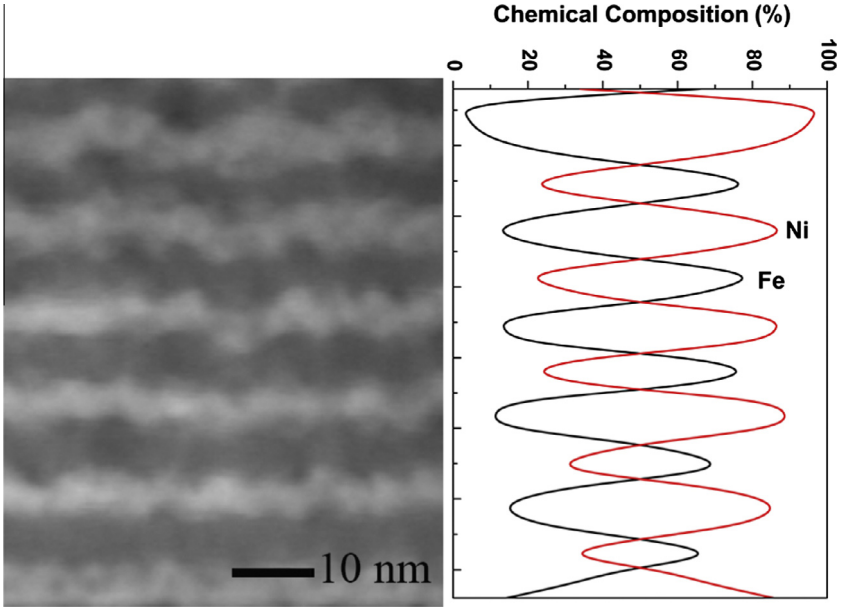

Fig. 2. Cross-sectional TEM micrograph and EDX line-scan analysis of the $[Fe(5\ nm)/Ni(5\ nm)]_{10}$ multilayers.

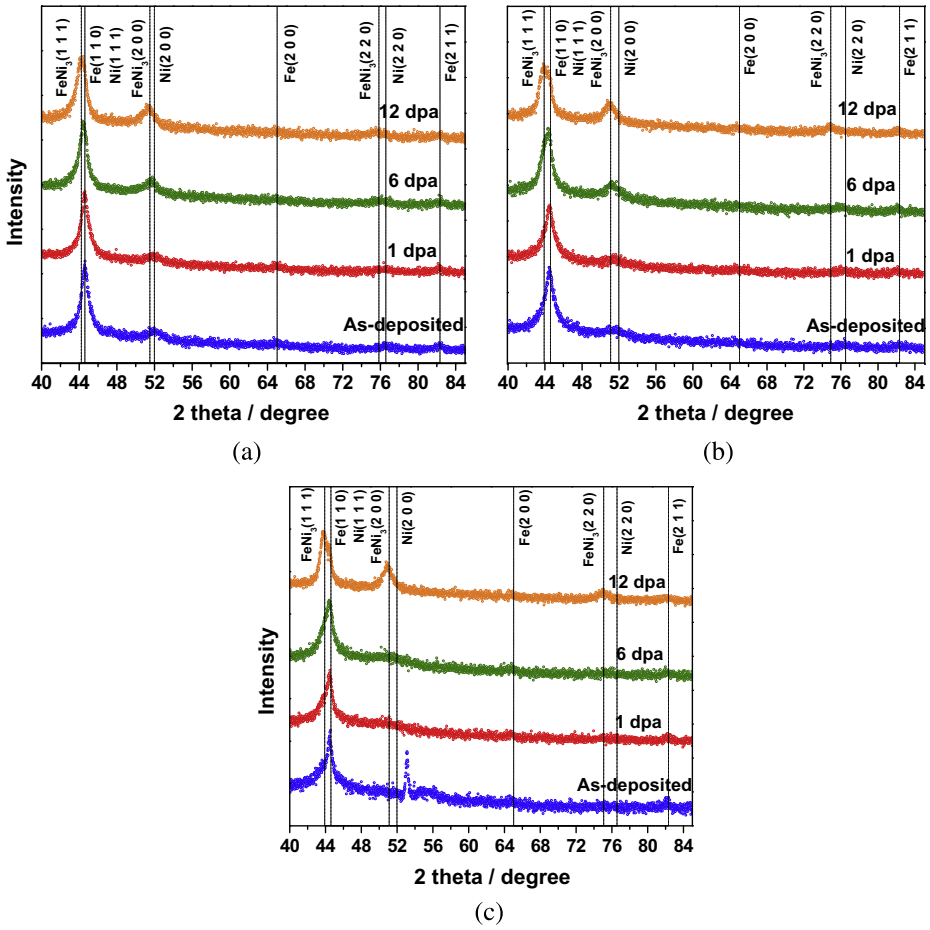

Fig. 3. GIXRD curves for Fe/Ni multilayers as a function of dpa. The acquisition rate was 5°/min. (a) $[Fe(10\ nm)/Ni(10\ nm)]_5$, (b) $[Fe(5\ nm)/Ni(5\ nm)]_{10}$, and (c) $[Fe(2\ nm)/Ni(2\ nm)]_{25}$.

$[Fe(5\ nm)/Ni(5\ nm)]_{10}$, and 12 dpa curve of $[Fe(2\ nm)/Ni(2\ nm)]_{25}$. $[Fe(2\ nm)/Ni(2\ nm)]_{25}$ does not exhibit distinct change up to 12 dpa; however, the shift degree is more violent compared with the 12 dpa curves of the other two samples. After ion irradiation, the shifted peaks located at 2θ values of 44.216°, 51.516°, and 75.842°, which are very close to the positions for $FeNi_3(111)$, $FeNi_3(200)$, and $FeNi_3(220)$, respectively. Although the peaks corresponding to the $FeNi_3(111)$ phase overlap with Fe(110) and

Ni(1 1 1) peaks, the other two observed peaks of $FeNi_3$ strongly indicate the formation of the $FeNi_3$ alloy phase. Thus, $FeNi_3$ is suggested to be formed during irradiation because of Fe and Ni intermixing driven by a negative mixing enthalpy. The formation of the metallic compound will be delayed as the modulation period of the multilayers decreases. However, the reaction will be more thorough once the metallic compound is formed.

Fig. 4 shows the cross-sectional micrographs and SAED pictures of multilayer before and after the irradiation. Fig. 4(a) and (b) represent the $[Fe(5\ nm)/Ni(5\ nm)]_{10}$ samples before the irradiation, while Figs. 4(c) and 2(d) represent the samples irradiated to 6 dpa.

Comparing Fig. 4(a) and (c), we can both discern the Fe/Ni interface from it, and the thickness of the single layer is about 5 nm. Obvious fluctuation was observed in Fig. 4(c), which represented the sample after irradiation. However, no further significant changes between the pre-irradiation sample and the post-irradiation one can be found. According to Fig. 4(b) and (d), we computed the interplanar spacing of the brightest diffraction ring. The spacing is about 2.051 Å. This conclusion is in accord with the result getting from the previous GIXRD measurement, since the spacing of Fe(1 1 0) and Ni(1 1 1) are 2.041 Å and 2.030 Å, respectively. After ion irradiation, the trend that the diffraction ring getting widen can be clearly observed from Fig. 4(d), indicating that the multilayer changed from polycrystalline to amorphous. However, the brightest diffraction ring remains the same in the whole process. Because of the minute variations between Fe(1 1 0), Ni(1 1 1) and $FeNi_3$(1 1 1), it's still hard to confirm the formation of $FeNi_3$ phase.

Veres et al. [17] proposed another interpretation for the shift phenomena of Fe(1 1 0) and Ni(1 1 1) peaks. As suggested by Veres, the shift indicates that the average Ni lattice parameter in the growth direction increases with the ion irradiation dose, which may be a sign of swelling. However, we did not adopt this interpretation because this observation can only analyze the shift qualitatively and cannot describe the precise location of the shifted peaks. Moreover, Veres and Gupta et al. [17,18] reported that the grain coarsening effect can be observed from GIXRD patterns. However, no peak can be selected to calculate the grain size in the present work because the Fe(1 1 0), Ni(1 1 1), and $FeNi_3$(1 1 1) peaks are overlapping while the other peaks are not intense enough.

Fig. 5 presents the GIXRD patterns of the 6 dpa curves of $[Fe(2\ nm)/Ni(2\ nm)]_{25}$ as a function of temperature during irradiation. A similar shift tendency can be observed from raising temperature during irradiation compared with the effects induced by increasing irradiation. Combining these curves with the curve of 12 dpa, the shift effect of 12 dpa irradiation at room temperature is between the effect of 6 dpa irradiation at 450 °C and 600 °C. In this view, irradiation at higher temperature facilitates the formation of metal compounds.

3.3. Magnetic properties

In the process of VSM testing, external magnetic field H that is applied to the multilayers is parallel to the surface of the films. The magnetic hysteresis loops of Fe/Ni multilayers resulting from various Fe^{10+} ion fluencies are shown in Fig. 6. Saturation magnetization M_s obviously increases with Fe^{10+} ion fluencies. Similar results were also reported by Bajalan et al. [19] and Gupta et al. [18]. The increase may be attributed to the formation of $FeNi_3$ alloy phase

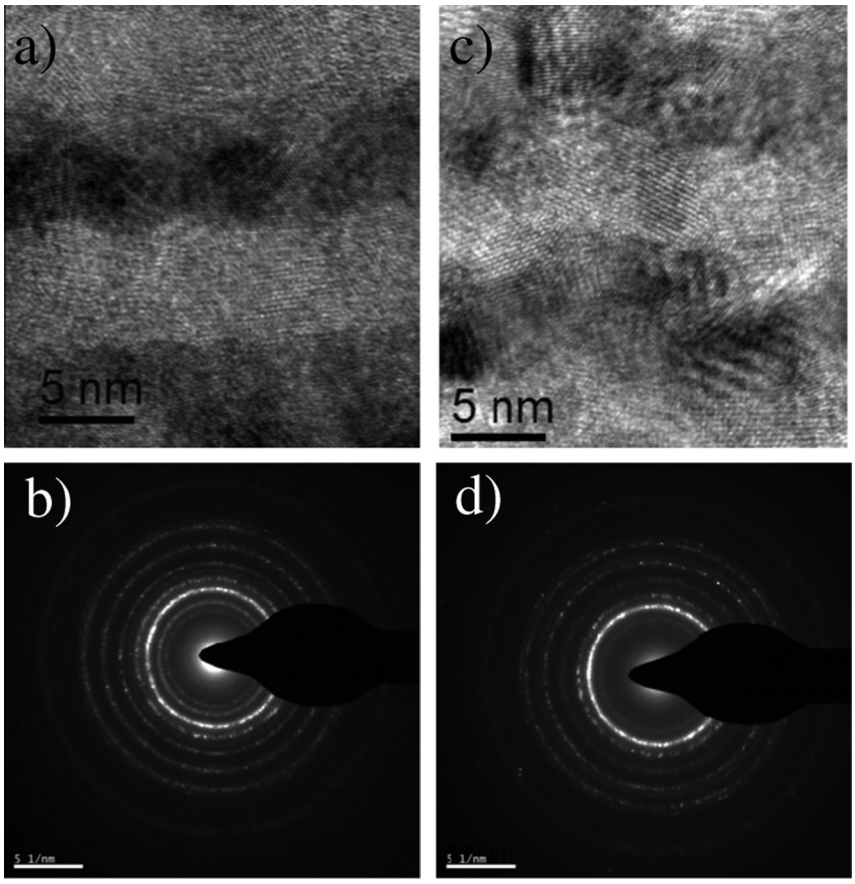

Fig. 4. Cross-sectional micrographs and the SAED pictures of the multilayer before and after ion irradiation: (a) cross-sectional micrographs of the as-deposited $[Fe(5\ nm)/Ni(5\ nm)]_{10}$, (b) SAED of the as-deposited $[Fe(5\ nm)/Ni(5\ nm)]_{10}$, (c) cross-sectional micrographs of the 6 dpa $[Fe(5\ nm)/Ni(5\ nm)]_{10}$ and (d) SAED of the 6 dpa $[Fe(5\ nm)/Ni(5\ nm)]_{10}$.

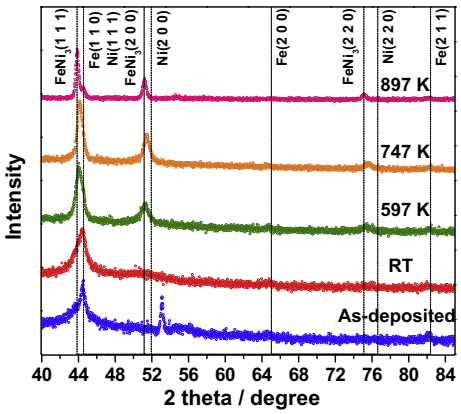

Fig. 5. GIXRD curves for [Fe(2 nm)/Ni(2 nm)]$_{25}$ multilayers with 6 dpa as a function of temperature during irradiation.

Table 1
Magnetic parameters of Fe/Ni multilayers determined from the loops.

Dpa	M_s (emu)	H_c (kOe)	M_r/M_s (%)
[Fe(10 nm)/Ni(10 nm)]$_5$			
As-deposited	0.0066	0.1449	30.44
1 dpa	0.0110		64.35
6 dpa	0.0110		68.08
12 dpa	0.0120		70.63
[Fe(5 nm)/Ni(5 nm)]$_{10}$			
As-deposited	0.0126	0.1373	69.05
1 dpa	0.0114		66.32
6 dpa	0.0124		69.22
12 dpa	0.0131		67.07
[Fe(2 nm)/Ni(2 nm)]$_{25}$			
As-deposited	0.0062	0.0148	60.41
1 dpa	0.0080		63.09
6 dpa	0.0095		63.80
12 dpa	0.0097		66.67

induced by ion bombardment, as indicated by the XRD results. However, different from most previous studies, the present study showed unchanged coercivity force H_c in the samples during the entire irradiation process. The parameters saturation magnetization M_s, coercivity force H_c, and remanence ratio (M_r/M_s) were determined from the loops. These parameters are tabulated in Table 1.

Considering the hysteresis loops of the three multilayers, [Fe(10 nm)/Ni(10 nm)]$_5$, [Fe(5 nm)/Ni(5 nm)]$_{10}$, and [Fe(2 nm)/Ni(2 nm)]$_{25}$, we noted a strong influence of modulation period on the saturation magnetization M_s. In the case of [Fe(10 nm)/Ni(10 nm)]$_5$, M_s that correlates to 1 dpa rises to the maximum rapidly and slightly changes with further increase in ions fluencies. Irradiation effects can be diminished distinctly when modulation period decreases to 5 nm [Fig. 6(b)]. However, better stability of M_s cannot be found in the case of multilayers with 2 nm modulation period. This result is different from that of previous studies of multilayers with immiscible interfaces mainly because of grain coarsening and Fe/Ni multilayer instability.

The behavior of the Fe/Ni multilayers under the co-influence of high temperature and ion irradiation was also investigated. Five curves of hysteresis loop of [Fe(2 nm)/Ni(2 nm)]$_{25}$ multilayers irra-

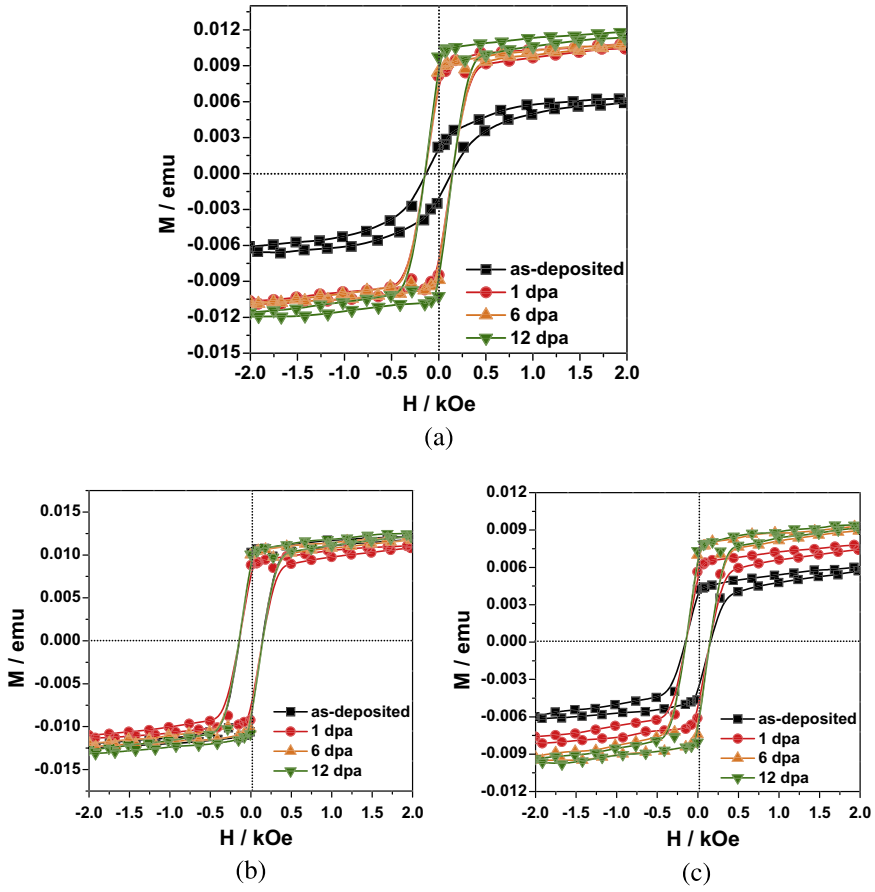

Fig. 6. Hysteresis loop of Fe/Ni multi-layers (ML), magnetic field parallel to samples: (a) [Fe(10 nm)/Ni(10 nm)]$_5$ ML; (b) [Fe(5 nm)/Ni(5 nm)]$_{10}$ ML and (c) [Fe(2 nm)/Ni(2 nm)]$_{25}$ ML.

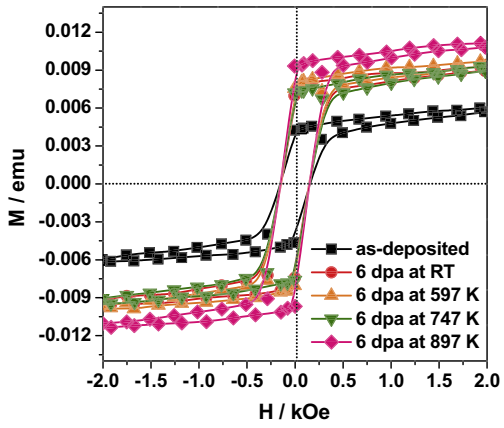

Fig. 7. Hysteresis loop of $[Fe(2\ nm)/Ni(2\ nm)]_{25}$ ML irradiated to 6 dpa at different temperatures, magnetic field parallel to samples.

diated to 6 dpa at different temperatures are represented in Fig. 7. Similar to the irradiation effects, M_s increases with increasing temperature. The manner by which ion irradiation and temperature interact with multilayers is almost the same, i.e., through a means called thermal spike model [20]. When high-energy ions are implanted into the materials, the deposition energy leads to local high temperature, which can be attributed to intermixing at the interfaces.

4. Conclusion

The effects of 300 keV Fe^{10+} irradiation on the structural and magnetic properties of Fe/Ni multilayers were investigated in this work. The formation of intermetallic compound can be attributed to the negative mixing enthalpy of the Fe/Ni system. After ion irradiation, coercivity force slightly changes but saturation magnetization increases rapidly. Unlike multilayers with immiscible interfaces, Fe/Ni multilayers with 5 nm modulation period show the highest stability of structural and magnetic performance.

Acknowledgements

This work was supported by the Specialized Research Fund for the Doctoral Program of Higher Education of China (SRFDP) (Grant No. 20133218110023), the Funding of Jiangsu Innovation Program for Graduate Education and the Fundamental Research Funds for the Central Universities (CXZZ13_0159), and Fundation of Graduate Innovation Center in NUAA and the Fundamental Research Funds for the Central Universities (Grant No. kfjj20130217). The irradiation experimental work was performed at the 320 kV platform for multi-discipline research, with highly charged ions at the Institute of Modern Physics, CAS. We wish to acknowledge the help of Kan Zhou during the preparation of multilayers and the help of Jingyu Li, Huiping Liu, Jingda Li, Long Kang, and Huan Li during the ion irradiation experiments.

References

[1] I. Ďuran, L. Viererbl, V. Klupák, I. Bolshakova, R. Holyaka, Czech. J. Phys. 56 (2006) B54–B60.
[2] K. Miyata, K. Miya, IEEE. T. Magn. 24 (1988) 230–233.
[3] T. Höchbauer, A. Misra, K. Hattar, R.G. Hoagland, J. Appl. Phys. 98 (2005) 123516.
[4] M.J. Demkowicz, R.G. Hoagland, J. Nucl. Mater. 372 (2008) 45–52.
[5] D. Bhattacharyya, M.J. Demkowicz, Y.Q. Wang, R.E. Baumer, M. Nastasi, A. Misra, Microsc. Microanal. 18 (2012) 152–161.
[6] L. Zhang, M.J. Demkowicz, Appl. Phys. Lett. 103 (2013). 061604–061604-4.
[7] M.G. Mcphie, L. Capolungo, A.Y. Dunn, M. Cherkaoui, J. Nucl. Mater. 437 (2013) 222–238.
[8] Q.M. Wei, N. Li, N. Mara, M. Nastasi, A. Misra, Acta. Mater. 59 (2011) 6331–6340.
[9] Yuan Gao, Tengfei Yang, Jianming Xue, Sha Yan, Shengqiang Zhou, Yugang Wang, J. Nucl. Mater. 413 (2011) 11–15.
[10] Kongfang Wei, Zhiguang Wang, Chunbao Liu, Hang Zang, Cunfeng Yao, Yanbin Sheng, Yizhun Ma, Yin Song, Lu Ziwei, Chinese Phys. C 32 (2008) 262–264.
[11] Akira Takeuchi, Akihisa Inoue, Mater. Trans. 46 (2005) 2817–2829.
[12] Mitch Jacoby, Chem. Eng. News 87 (2009) 14–18.
[13] J.F. Ziegler, M.D. Ziegler, J.P. Biersack, Nucl. Instrum. Meth. B 268 (2010) 1818–1823.
[14] Rudy Konings, Comprehensive Nuclear Materials, Newnes, OnlineVersion, 2012. pp. 3–4.
[15] P.J. Sadashivaiah, T. Sankarappa, T. Sujatha, R. Ramanna, Int. J. Mater. Res. 1 (2013) 272–278.
[16] S.K. Srivastava, Ravi Kumar, A. Gupta, R.S. Patel, A.K. Majumdar, D.K. Avasthi, in: Nucl. Instrum. Meth. B 243 (2006) 304–312.
[17] T. Veres, M. Cai, R.W. Cochrane, M. Rouabhi, S. Roorda, P. Desjardins, Thin Solid Film 382 (2001) 172–182.
[18] Rachana Gupta, Ajay Gupta, Appl. Surf. Sci. 238 (2004) 254–261.
[19] D. Bajalan, H. Hauser, P.L. Fulmek, Wiener Neustadt (2005) 140–143.
[20] C. Weissmantel, K. Bewilogua, D. Dietrich, H.J. Erler, H.J. Hinneberg, S. Klose, W. Nowick, G. Reisse, Thin Solid Film 72 (1980) 19.